Journal of The Electrochemical Society, **153** (10) D155-D161 (2006)
0013-4651/2006/153(10)/D155/7/$20.00 © The Electrochemical Society

Effects of Process Conditions on Properties of Electroplated Ni Thin Films for Microsystem Applications

J. K. Luo,[a] M. Pritschow,[b] A. J. Flewitt,[a] S. M. Spearing,[c,*] N. A. Fleck,[a] and W. I. Milne[a]

[a]*Department of Engineering, University of Cambridge, Cambridge CB3 0FA, United Kingdom*
[b]*Institute for Microelectronics Stuttgart, 70569 Stuttgart, Germany*
[c]*School of Engineering Science, University of Southampton, Southampton SO17 1QJ, United Kingdom*

The properties of electroplated Ni thin films have been systematically investigated as a function of plating temperature and current density. The resistivity and its temperature coefficient remain unchanged on varying the process conditions, though the values of these properties are approximately three times and one-half of those of bulk Ni material, respectively. Optimal conditions of $J = 2$ mA/cm^2 and 60°C were found for stress-free Ni thin films. The modulus of elasticity of the Ni films is as high as that of bulk Ni (210 GPa) when plated at high temperature and low current density, and then decreases linearly with increasing plating current density, down to 85 GPa at a plating current density of 30 mA/cm^2. It is believed that higher plating rates produced fine-grained structures of low density, leading to a high tensile stress and low modulus of elasticity, while lower plating rates produced a dense material with a modulus of elasticity close to that of bulk Ni and a compressive residual stress. A clear correlation between modulus of elasticity and the stress exists, which reveals that a material under high tensile stress may posses a low modulus of elasticity, and is not suitable for fabrication of microelectromechanical systems devices.
 [DOI: 10.1149/1.2223302]

Manuscript submitted March 6, 2006; revised manuscript received May 24, 2006. Available electronically July 26, 2006.

Although current microelectromechanical systems (MEMS) technologies are dominated by standard complementary metal oxide semiconductor (CMOS) compatible materials and silicon-microelectronics processes, there is interest in expanding the material and process sets to include micromachined metals and polymers,[1,2] as they have the potential to provide greater functionality and performance, and to reduce manufacturing cost. Electroplating metal films may play an important role in MEMS technology, as it provides an easy, simple, and low-cost technology for MEMS device development with comparable mechanical properties to the silicon-based material set, while offering an enhanced set of properties for transducers. Sensors and actuators based on plated metals have been fabricated and studied, including thermal actuators, microcoils, micromotors, and pneumatic actuators.[3-11] Ni and NiFe are the electroplated metals most commonly used for MEMS devices.[3-9] Stress-free deposited layers are essential for MEMS applications, in order to allow for dimensional control and linear transducer responses. This is particularly important in thin layers, where even small stresses or stress gradients can result in large, out of plane deflections. The residual stress in metal-plated films has been studied by a number of research groups, but research has concentrated mainly on thick metal films.[12-16] The stress for plated thin films is expected to be different from that of thick materials, and it is important to clarify the relationship between residual stress and plating conditions.

From the design and fabrication point of view, other material properties such as the temperature coefficient of the resistivity and the modulus of elasticity (also called Young's modulus) are particularly important. Although a large amount of work has been done on electroplated Ni, especially thick films, and data for resistivities, stress, and Young's modulus are available,[12-20] it lacks a systematic investigation. Commonly, MEMS devices are first designed according to closed-form analysis, the structures are then simulated and optimized by finite-element analysis, and finally they are fabricated, characterized, and compared to the simulations. The bulk properties are often used for MEMS design and modeling. However, the resulting device performance after fabrication can be very different from the predicted performance due to the dependence of the properties of plated thin metals upon processing. This leads to redesign and refabrication of MEMS devices, increasing the development time and cost. Surprisingly, the properties of electroplated Ni films, which are very important materials for MEMS applications, and their relationship with process conditions have not been clarified. In this paper, we report the detailed investigation of the effect of the plating process conditions on the electrical and mechanical properties of electroplated Ni thin films including residual stress, the resistivity and its temperature coefficient, and the modulus of elasticity. A correlation between residual stress and the modulus of elasticity of the film is established.

Experimental

Plating bath and solution.— The electroplating solution was commercially purchased nickel sulfamate solution (Celtic Chemicals Ltd.) with specific contents ordered as shown in Table I. The pH value of the plating solution was 3.8 initially, and then increased to ~5.0 after 100 h of plating. The plating bath was purpose-built and consisted of a hot water bath, a bottle for the plating solution with a lid to prevent vaporization of the solution (with two electrodes inserted through it), a circuit to control the current, and a Ni anode electrode with an area of ~4 cm^2. A magnetic pellet was used to stir the solution at a speed of 1000 rpm to keep the concentration uniform and to prevent the formation of hydrogen bubbles on the sample surface, which could lead to pits in the film. The plating temperature was adjusted in the range of 20–80°C with ±2°C accuracy, and the current density was adjusted in the range of 1–30 mA/cm^2. For all experiments reported here, the pH value of the solution was not adjusted as the experiments were conducted in a very short time span.

Sample preparation.— Chromium and copper seed layers with thicknesses of 5 and 60 nm, respectively, were deposited on the Si substrate by sputtering (CRC sputtering system). The Cr interlayer was used to increase the adhesion between the Cu seed layer and the Si substrate. Ni was plated on to a plain Cu seed layer for residual stress investigation with a typical thicknesses of 0.4–0.7 μm (it forms a bilayer with the Si substrate). For the beam bending experiments to extract the modulus of elasticity, large single Ni layer cantilever beams were used. Ni thin films with a typical thickness of 1.5–3 μm were first plated, and then cantilevers were defined by

Table I. Nickel sulfamate solution.

Nickel sulfamate	$Ni(SO_3NH_2)_2 \cdot 4H_2O$	300 g/L
Nickel chloride	$NiCl_2 \cdot 6H_2O$	10 g/L
Boric acid	H_3BO_3	40 g/l

* Electrochemical Society Active Member.

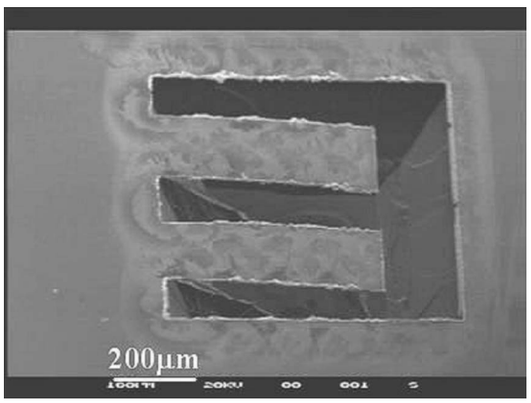

Figure 1. An SEM picture of a Ni cantilever made by laser micromachining and KOH etching. The cantilever has a length, width, and thickness of 500 × 150 × 2.5 μm.

laser micromachining (New Wave Research, laser machining system mode PXC). Thicker Ni films were used for beam bending experiments so as to avoid large deflection. A multipass UV light (λ = 355 nm) laser was used to cut through the thick Ni films. Because the laser pulse is short (3 ns, 10 Hz) and the thermal conductivity of Ni is very good, the damage by localized heat of the laser pulse is restricted on the edge of the cantilever. This does not affect the integrity of the cantilever as it is much smaller compared to the size of the cantilever. The beam had a length and width of 500 and 150 μm, respectively. Ni beams were then released by KOH etching at 85°C, using a 20% by weight aqueous solution, to remove the Si underneath the beams with a typical etching time of 90 min. Figure 1 is the scanning electron microscope (SEM) picture of a fabricated cantilever. The thickness of the Ni film was carefully measured by a Dektak profilometer and SEM, and the average value was used for the extraction of Young's modulus.

For resistivity measurements, Ni wire test structures with bond pads were made by a through-mask plating technique on SiO_2/Si substrates,[21] using positive photoresist AZ5412 ($d \sim 1.4$ μm) as the plating mold. The metal thickness for this experiment was 0.3–1 μm. After plating, the photoresist was removed by dissolving in acetone, and the seed layer outside the test structures was etched by chromium etchant and rinsed in deionized (DI) water. The typical beam width was 6 μm with length varying from 360 to 580 μm. These Ni beams were not released from the substrates. The dimensions were carefully measured and the average values were used for the resistivity calculation, due to the nonuniformity of the plated narrow structures.[22]

Measurements.— Plated Ni layer forms a bilayer structure with the Si substrate. If residual stress exists, then it causes the bending of the bilayer structure. From the bending, it is possible to extract the residual stress. The residual stress consists of a mean stress, which acts along the uniaxial direction, and a stress gradient. The mean stress contributes to the curvature of the bilayer specimen, and it does not affect the curvature of a freestanding cantilever significantly if the magnitude of the stress is small,[23] while the stress gradient affects the curvature of a bilayer structure as well as a freestanding cantilever. Therefore, the measured total residual stress from a bilayer structure includes mean stress and stress gradient. When the film thickness is much smaller than that of the substrate, the total stress σ_t, of a plated Ni film can be related to the curvature of a bilayer structure by Stoney's equation[24]

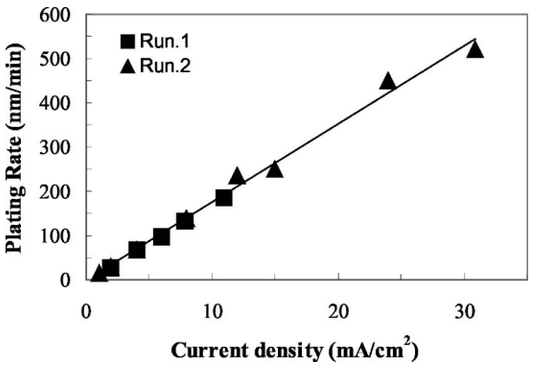

Figure 2. Ni electroplating rate linearly increases with the current density at a fixed plating temperature of 60°C.

$$\sigma_t = \frac{E_s t_s^2 \kappa}{6(1-\nu_s)t_f} \quad [1]$$

E_s is the Young's modulus of the Si substrate, ν_s the Poisson's ratio, t_s and t_f the thickness of the Si substrate and the Ni film, respectively, and κ is the curvature of the bilayer structure. The curvatures of specimens before and after Ni plating were measured by a DekTak-8 profilometer with a scan distance of >1 cm, and the differences were extracted to calculate the residual stress. Several curvatures were measured and the average values used here.

The DekTak-8 was also used to conduct a beam-bending experiment to deduce the modulus of elasticity of the Ni films with a force in the range of 1–100 μN with details explained in Ref. 25 and 26.

The resistances of test structures were measured at various temperatures from 20 to 250°C on a probe station with a hotplate stage. Probes were directly contacted onto the bond pads, and were connected to a dc voltage source, which was controlled by a computer. The measured resistance includes contributions from the probe contact and the bond pads. In order to eliminate these contributions, resistances were measured from a series of beams with different lengths. The resistance of the beams was extracted from the slopes of R vs L plots.

Results

Plating rate.— According to Faraday's law, the plating rate is proportional to the current density.[14] The experimental results (Fig. 2) showed a linear relationship between the plating rate, γ, and the current density, J. It can be expressed as

$$\gamma = 17.6J \text{ (nm/min)} \quad [2]$$

Here, J is in units of mA/cm^2. The current efficiency which is defined as the ratio of the current used for the reduction of the ions for the intended deposit to the total current passed through the devices,[27] was found to be ~94%, indicating that hydrogen inclusion in the film is very limited. The temperature has a very limited effect on plating rate for $T \leq 60$°C; it remains almost unchanged with a scatter of ~15% for a fixed current density. But, the plating rate at 80°C was found to increase by more than 50%. This is believed to be caused by the onset of hydrolysis at this temperature, which introduces ammonium and sulfur in the film, leading to a drastic increase in plating rate.[12]

Resistivity and its temperature coefficient.— Resistivity and its temperature coefficient, ξ, are important parameters for MEMS development. ξ of electroplated Ni films is expected to be different from that of bulk material, as the material's microstructure and impurity density are different from those of bulk Ni. The resistivities of the samples plated at $J = 2$ to 30 mA/cm^2 are in the range of 17–22 μΩ cm as shown in Fig. 3. Although the data are scattered,

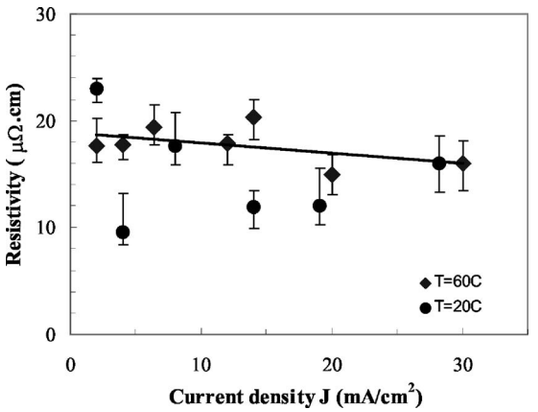

Figure 3. Resistivity as a function of plating current density. Although the data have a large scatter, it remains almost unchanged with plating current density.

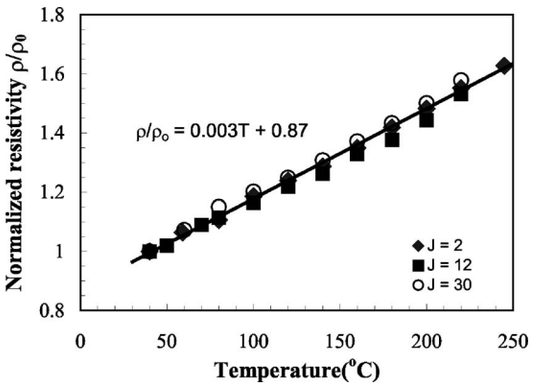

Figure 5. The normalized resistivity as a function of measurement temperature for three samples plated at 2, 12, and 30 mA/cm^2 (T = 60°C). They showed a similar temperature coefficient of resistivity.

this value does not vary significantly with current density. The average resistivity for these samples is about three times that of the bulk value of 6.85–7.78 μΩ cm.[18,28,29]

Figure 4 shows a typical plot of resistance, $R(T)$, vs temperature for samples plated at 12 mA/cm^2 and 60°C. It increases linearly with increasing temperature up to 250°C. In order to obtain the temperature coefficient of resistivity, $\rho(T)$, the resistance is normalized according to

$$\frac{R(T) - R_o}{R_o} = \frac{\rho(T) - \rho_o}{\rho_o} = \xi T \qquad [3]$$

Here, R_o and ρ_o are the room temperature resistance and resistivity. Figure 5 shows the normalized resistivity $\rho(T)/\rho(T_0)$, plotted against the temperature. These samples were plated at J = 2, 12, and 30 mA/cm^2, respectively, at a fixed plating temperature T = 60°C. The resistance of Ni thin films increases with the measurement temperature linearly for all samples, with a converged temperature coefficient of $(3.0 \pm 0.3) \times 10^{-3}$/°C, about half that of the bulk value of 6×10^{-3}/°C.[30] It is clear that up to 250°C, the resistivity of plated Ni films is linear with temperature, and higher order terms are not required to fit the data. Despite a wide range of plating current density, the temperature coefficient of resistivity remains essentially constant. These results of resistivity and its temperature coefficient have demonstrated that the plating conditions have limited effects on the electrical properties of the Ni films.

An increase in resistivity in a thin film is normally observed, especially when the film thickness approaches the grain size, as this interrupts the conduction path. Plated materials are not as pure as bulk materials; therefore, a higher resistivity for a plated material is normal. This has been observed for electroplated Cu films for IC applications[31] and other materials.[29] It was also found that the resistivity increased quickly as the plating solution ages in the present work, and it increased by more than 100% when plated at 80°C, corresponding to the inclusion of organic elements and porous structure as discussed later.

Total residual stress.— Figure 6 shows the dependence of the total stress on the plating temperature, in the range of 20 to 80°C at a fixed current density of 2 mA/cm^2. At low temperatures the plated films are compressively stressed, and become progressively more tensile with increasing temperature, changing from compressive to tensile at a temperature of ~60°C. The residual stress shows a linear relationship with plating temperature that can be fitted by

$$\sigma_t(T) = 6.6T - 393 \text{ (MPa)} \qquad [4]$$

Here, T is in the unit of degrees.

Figure 7 shows the dependence of the total stress of Ni films on the plating current density at a temperature of 60°C, with the top axial showing the corresponding plating rate calculated by Eq. 2 for these films. The general tendency shows that the stress changes from compressive to tensile, and the magnitude increases with increasing current density. Low current density plating produces a compressive

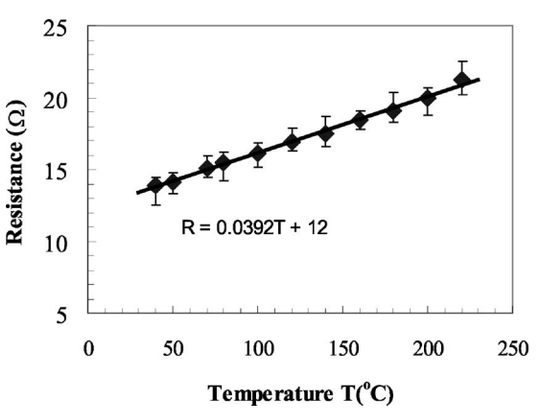

Figure 4. Resistance as a function of measurement temperature for a Ni film plated at 12 mA/cm^2 and 60°C. It increases linearly with increasing temperature.

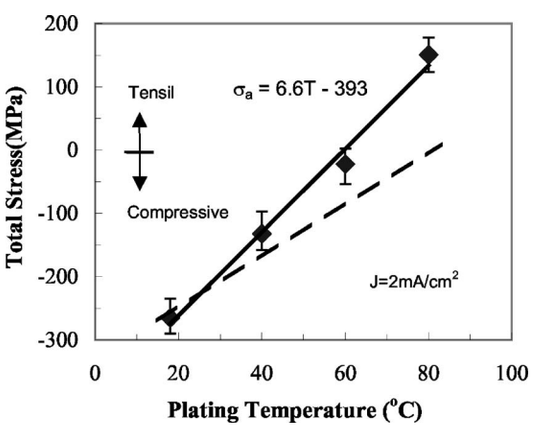

Figure 6. The dependence of the total stress on the plating temperature at a fixed current density of 2 mA/cm^2. The dashed line is the intrinsic stress after extracting the thermal tensile stress.

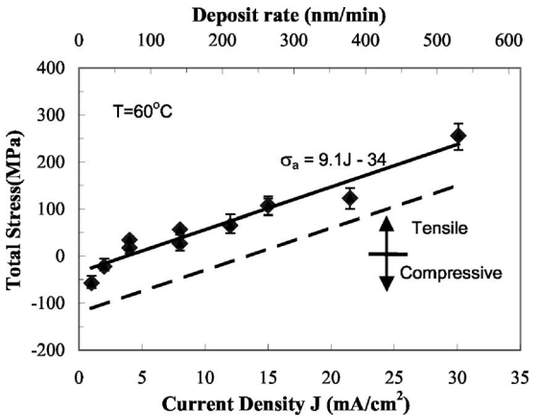

Figure 7. The dependence of the total stress on the plating current density at a fixed temperature of 60°C. Dashed line is the intrinsic residual stress after extracting the thermal stress.

stress, while a high current density plating produces a tensile stress. Obviously a zero stress regime therefore exists. This result is comparable to observations by others.[12] The total stress has a linear relationship with the plating current density as follows

$$\sigma_t(J) = 9J - 34 \text{ (MPa)} \quad [5]$$

Here, J is in the unit of mA/cm^2. The gradient of Eq. 5 was found to depend on the temperature, and it decreases with decreasing temperature. Therefore, the total stress expressed as a function of temperature and current density is not a simple linear combination of Eq. 4 and 5. More experiments are needed to extract a complex form for the total stress.

A Ni film plated on a Si substrate at an elevated temperature is subjected to a tensile stress due to the difference between the thermal expansion coefficients, α, of the Ni ($\alpha_{Ni} = 12.7 \times 10^{-6}$/°C) and the Si substrate ($\alpha_{Si} = 2.5 \times 10^{-6}$/°C). The generated thermal tensile stress σ_{TH} is given by

$$\sigma_{TH} = (\alpha_{Si} - \alpha_{Ni})(T - T_o)E_f \quad [6]$$

Here, T_o is the room temperature.

The measured residual stress includes thermal and intrinsic stresses. The intrinsic stress may be generated due to the inclusion of impurities and defects, boundary relaxation, etc. The thermal stress is linearly related to temperature by Eq. 6. By subtracting the thermal tensile stress, a net intrinsic stress can be obtained as shown in Fig. 6 by the dashed line. It is clear that the intrinsic stress is dominated by the compressive stress over the plating temperature range investigated, while the tensile stress in the films plated at low current density is caused by the extrinsic thermal stress. The intrinsic stress is nearly zero when it is plated at 80°C, and increases linearly with decreasing temperature. Similarly, the intrinsic stress after subtracting the thermal stress has been calculated for those films plated at different current densities at 60°C and is shown in Fig. 7 by the dashed line. This reveals that the intrinsic stress for Ni films plated at a current density <15 mA/cm^2 is compressive, while those plated at a higher current density exhibit a tensile stress. As before, therefore, a zero-stress regime exists.

Plating at an elevated temperature is commonly used to minimize the residual stress. High-temperature plating enhances the relaxation of the plated Ni atoms, thus leading to a low stress in the films. A long relaxation time at a fixed temperature is essential to obtain a low-stress film. This has been achieved in commercial systems by using pulse mode plating, which effectively increases the time for stress relaxation to occur, resulting in significant reductions in stress.[13,32]

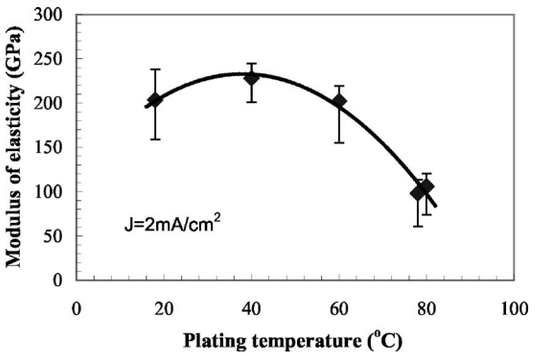

Figure 8. Modulus of elasticity as a function of plating temperature. E drastically drops to half of the bulk value; the enclosure of organic specimen by hydrolysis is believed to be responsible for it.

Modulus of elasticity.— Many efforts have been made to extract the modulus of elasticity of thin films, as it is very important for MEMS design and fabrication.[33-35] However, the scatter of modulus of elasticity of a material remains very large even by the same method. Undercutting of the beam induced by wet etching is one factor affecting the accurate extraction of the modulus of elasticity when a freestanding beam is used, but the effect is not significant. Finite-element modeling has confirmed that the error in extracting E due to undercut is less than 1% when the undercut length is less than 10% of the beam length.[25] The extracted modulus of elasticity from these Ni films is shown in Fig. 8 as a function of plating temperature. For temperature in the range of 20–60°C, the modulus of elasticity does not change significantly and is close to the bulk value of 210 GPa for Ni metal. A high value of $E_f = 228 \pm 15$ GPa was obtained, but is still believed to be within the experimental scatter. The modulus of elasticity drops to ~100 GPa at 80°C, half of the bulk Ni value. The dramatic reduction of the modulus of elasticity at 80°C has been reproduced in repeat experiments, confirming that it is not due to experimental scatter.

This reduction of E at 80°C has been attributed to the formation of sulfate and ammonium ions at $T > 70$°C due to hydrolysis.[12] Inclusion of organics species increases the resistivity and modifies the mechanical properties.[29,36] It is expected that the enclosure of these nonmetallic species will change the microstructure and atomic arrangement of plated Ni, leading to a Ni film with a sufficiently high defect density that the stiffness is reduced. The plating rate for the 80°C samples was 50% higher than those at $T \leqslant 60$°C with the same current density, which is likely to result from some inclusion of other species in the Ni film. This is currently under investigation.

Figure 9 shows the dependence of modulus of elasticity on the plating current density in the range of 1 to 30 mA/cm^2 at T = 60°C. The modulus of elasticity decreases linearly from a near-bulk value of 205 to 85 GPa, on increasing the plating current density. Data obtained from Ref. 1 and 40 are shown in Fig. 9 for comparison, roughly in agreement with ours. This linear decrease of the modulus of elasticity is believed to be caused by changes in the microstructure, and is discussed later.

Effects on surface morphology.— SEM and atomic force microscopy (AFM) have been used to inspect the surface morphology and microstructure of the plated Ni films. The detailed study of the surface roughness of these electroplated Ni films can be found in Ref. 22, and the results are briefly highlighted here. Figure 10 shows SEM pictures from samples plated at 20, 60, and 80°C (a)–(c) (J = 2 mA/cm^2), and 15 and 30 mA/cm^2 (d)–(e) (T = 60°C), respectively. It is clear that the morphology of the Ni films changes significantly on varying the plating conditions. Low-temperature plating produces a rough surface with a large grain size and clear crystalline features. As the temperature increases, the surface gradually becomes smoother and the grain size decreases, leading to a

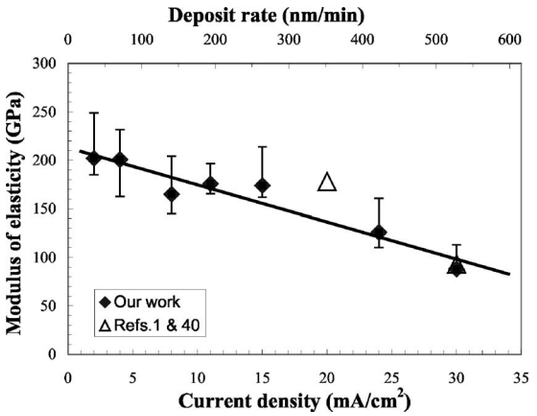

Figure 9. Modulus of elasticity as a function of plating current density. It linearly decreases with increasing current density.

featureless surface. Further increase in the plating temperature to 80°C leads to a drastic increase of the surface roughness as shown in Fig. 10c. It is clear that the Ni films become grainy with clear crystal orientations, and the grain size is on the order of 0.3–2 μm. At an optimal temperature of 60°C, the surface roughness of the Ni film was investigated as a function of current density. It was found that the roughness increases from ~10 nm with current density, reaches its peak of ~25 nm at $J \sim 15$ mA/cm^2, and then decreases with increasing the current density.[22] For simplicity, the sample plated at $J \sim 15$ mA/cm^2 with the roughest surface was chosen here. For detailed roughness investigation please refer to Ref. 22.

Discussion

Effect of microstructure on materials properties.— The electrical properties of Ni films do not change significantly on varying the plating conditions, while the mechanical and stress strongly depend on the process conditions. These behaviors seem contradictory, however; the resistivity and its temperature coefficient largely depend on the transportation of electrons in the metal film, while the mechanical properties depend on the integrity of a metal film and its microstructure, especially when the beam-bending test is used. Unlike in semiconductors, electrons can move freely in metals. The resistivity of a metal film will not change significantly as long as the dimension of the conductive path is much larger than the grain sizes. But the resistivity changes when the crystal structure changes from a polycrystalline to an amorphous structure, owing to the lack of periodicity in an amorphous structure. The observed results imply that the fundamental crystal structure does not change, but the grain sizes. Electroplated metal films were found typically to have large columnar polycrystalline structures when plated at high temperature and at low rates, and they become fine-grained structure as the current density increases.[29,37] This may be responsible for the relative constant resistivity of our plated Ni films observed. The resistivity obtained from our work is about three times of the bulk value and those obtained from the thick Ni films.[18] The reason may be twofold. The high resistivity is obtained from microfabricated test structures with a thickness of 0.4–0.7 μm. Surface roughness, grain size, surface oxidation, etc. will have a profound effect on it, but will not affect the electrical properties of bulk and thick films. Second, no specific procedure was taken to purify the solution used in our experiments; impurities enclosure may be responsible for the high value of the resistivities as observed by others.[29,36] The higher resistivity in the plated Ni films produced from an aged solution may well be explained because of this effect.

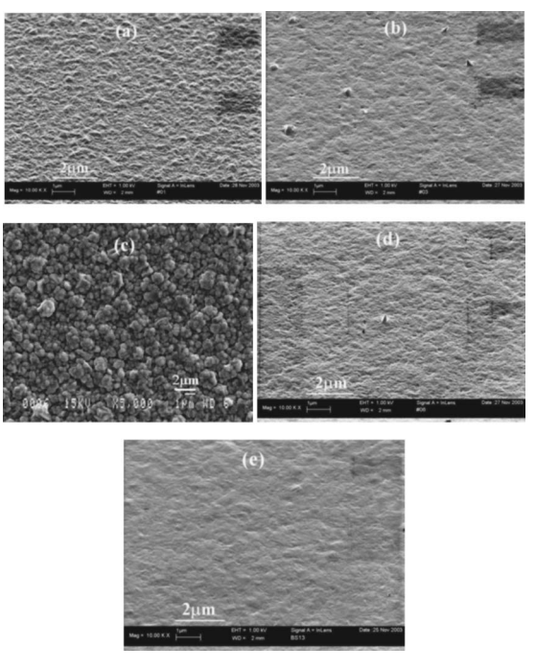

Figure 10. SEM pictures of Ni films plated at a $T = 20$, 60, and 80°C (a)–(c) at $J = 2$ mA/cm^2, and at $J = 15$ and 30 mA/cm^2 (d) and (e) at $T = 60$°C.

The zero-stress plating temperature, 60°C, is in agreement with that obtained in Ref. 12, but different from the 50°C obtained by others. From our work and those of Ref. 12, it is clear that the zero-stress plating temperature varies with the concentration, higher concentration, higher zero-stress plating temperature, and vice versa. It is believed that 10°C difference is still within the experimental scatter. The causes for intrinsic stress may include lattice mismatch between the substrate and plating material, inclusion of impurities and defects, and microstructure change. As all these experiments were conducted under similar conditions within a very limited time span, the changes in solution concentration and impurity density are expected to be small as evidenced by small change of the resistivity of the samples; therefore, they are not likely to be responsible for the intrinsic residual stress observed. Hydrogen bubbles or pits are also not likely to be responsible for the intrinsic stress as only few pits were found in the film by high-magnification SEM. In polycrystalline structures, mismatch makes no significant contribution to the stress generation as stress is relaxed in the boundaries.[38,39]

The variation of the intrinsic stress and the modulus of elasticity can be explained by the change of microstructure caused by the plating conditions. At low plating current density and optimal temperature of 60°C, the plating is limited by the reaction rate. There is a sufficient supply of Ni ions to the cathode, and the reduced Ni atoms have sufficient time to relax. The deposited Ni film is hence dense, strong, and with large columnar structures. It possesses a compressive stress with the characteristics of a polycrystalline phase. At high current density, the plating rate is high. Atoms may pile up with insufficient time to relax, and hence leave behind pores with relatively weak adhesion between grains in the film. The deposited layer is porous, with a fine-grained structure, possessing a tensile stress. This leads to a reduced material strength and the modulus of elasticity. Surface roughness study has shown that low current density produced a smooth Ni surface and the roughness increased as the plating current density increased to a modest range of current density, then it decreased until further increases in the current density. This corresponds to a change of grain structure from large polycrystalline to a fibrous, fine-grained structure. A low modulus of elasticity in thick Ni films produced by the LIGA process and electroplating has been reported. Values of 178 and 93 GPa using a sulfamate plating bath were obtained at $J = 20$ and 30 mA/cm^2, respectively,[1,40] and are comparable to what we have measured. The low modulus of elasticity was attributed to the fibrous grain structure.

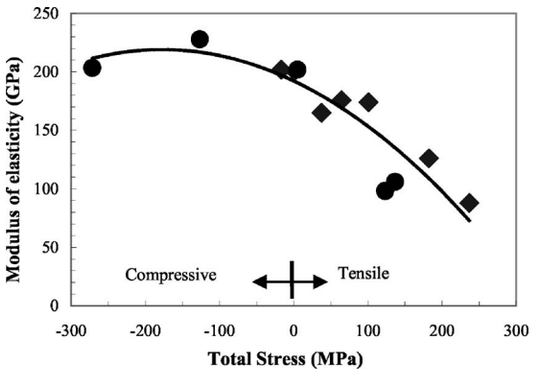

Figure 11. The modulus of elasticity of electroplated Ni films as a function of total stress. In the compressive stress range, the modulus of elasticity remains higher, close to that of bulk value, while in the tensile stress range, it decreases rapidly with increasing in tensile stress.

Temperature has a similar effect as the current density on the film properties. Plating at low temperature and low current density leads to a higher compressive stress (shown in Fig. 6 and 7) as atoms remain in the as-deposited locations due to the low migration rate. Increasing the plating temperature enhances the migration rate, and atoms can relax to the lower energy states, leading to a low stressed film. Further increase in the temperature to 80°C introduces an electrolysis process, which produces organic species in the solution. Metals are deposited in a rough form when the electrolysis occurs,[12] consistent with our observation as shown in Fig. 10c. The porous structure with large boundaries is believed to be responsible for the reduction in the modulus of elasticity.

Correlation between the stress and the modulus of elasticity.— As the modulus of elasticity and the residual stress both have a linear relationship with plating current density, and the stress is reproducible, it is reasonable to assume the total stresses of samples found from the stress and beam-bending experiments are the same when they are plated under the same conditions, and the stress can be calculated via Eq. 4 and 5 for those samples used in the beam-bending experiments. The modulus of elasticity extracted by varying the current density and temperature is replotted as a function of total stress in Fig. 11. Here, the measured total stress rather than the intrinsic stress is used, as the film's properties were determined during plating where the thermal stress does impose effect. Although the decrease of the modulus of elasticity was caused by different mechanisms (inclusion of organics and porosity), it has an identical trend with the stress. The results clearly imply that the modulus of elasticity for those deposited under a compressive stress remain higher, close to that of bulk material. When a film is deposited under tensile stress, the modulus of elasticity decreases with increasing magnitude of tensile stress, down to only half the bulk value at a tensile stress of 240 MPa. The results clearly indicate the modulus of elasticity of a film can be modified by the stress associated with its deposition process. Material under tensile stress during deposition is normally less dense, porous microstructure, while that under compressive stress during deposition is more dense, stronger, and harder material. This correlation is different from the strain-stress relationship, $\sigma = E\epsilon$. The former is a correlation of E associated with the process. Once the film is deposited, the strain-stress relationship still applies no matter what E value it has. This is particularly important for MEMS device design, as engineers tend to use tensile material as a membrane for MEMS devices, rather than compressively stressed material.[41,42] This is because membranes or bridges with compressive stress tend to buckle when they are released from the substrate, while tensile material can avoid this buckling. Our results, however, demonstrate that a tensile stressed material corresponds to a lower modulus of elasticity. It may be less dense, porous, and is likely to be less reliable for fabrication of MEMS devices.

Conclusions

The properties of electroplated Ni thin films have been systematically investigated as a function of plating temperature and current density in terms of temperature coefficient of resistivity, average residual stress, and the modulus of elasticity. The following conclusions can be drawn.

1. The intrinsic residual stress is dominated by compressive stress when it is plated at a low current density. The magnitude of the compressive stress increases with decreasing plating temperature. At a fixed temperature, the residual stress of a Ni thin film changes from a small compressive stress to a tensile value, and the magnitude increases with increasing plating current density.
2. The resistivity of plated Ni films does not change significantly with plating conditions, having a value three times that of the bulk value. The temperature coefficient of resistivity remains unchanged as the plating current density is varied by one order of magnitude. The temperature coefficient is 3×10^{-3}/°C, which is half that of the bulk Ni material.
3. The modulus of elasticity of Ni films remains high when plated at low temperature and low current density, but it drastically reduces to a value of 85 GPa, less than half that of the bulk value, when it is plated at 80°C. Inclusion of organic specimens produced by electrolysis at this high temperature is responsible for the reduction in the modulus of elasticity.
4. A correlation between the modulus of elasticity and the stress of the film during deposition was found. The modulus of elasticity remains as high as that of bulk when the film is deposited under a compressive stress, and decreases drastically when the film is deposited under severe tensile stress. High current density plating produces less dense, thin films, possessing high tensile stress, leading to the reduction of the modulus of elasticity, while slow plating produces dense and strong films with E close to that of the bulk value.

Acknowledgments

This research was partially sponsored by the Cambridge-MIT Institute under grant no. 059/P and by the EU FP6 program under the project name "PROMENADE."

References

1. S. D. Leith and D. T. Schwartz, *J. Microelectromech. Syst.*, **8**, 384 (1999).
2. P. Shao, Z. Rummler, and W. K. Schomburg, *J. Micromech. Microeng.*, **14**, 305 (2004).
3. J. Gobet, F. Cardot, J. Bergqvist, and F. Rudolf, *J. Micromech. Microeng.*, **3**, 123 (1993).
4. W. H. Teh, J. K. Luo, M. A. Graham, A. Pavlov, and C. G. Smith, *J. Micromech. Microeng.*, **13**, 591 (2003).
5. S. Majumder, N. E. McGruer, and P. Zavracky, *J. Vac. Sci. Technol. A*, **15**, 1246 (1997).
6. K. Kataoka, S. Kawamura, T. Itoh, K. Ishikawa, H. Honma, and T. Suga, *Sens. Actuators, A*, **A103**, 116 (2003).
7. T. Matsunaga, K. Kondoh, M. Kumagae, H. Kawata, M. Yasuda, K. Murata, and M. Yoshitake, *Jpn. J. Appl. Phys., Part 1*, **39**, 7115 (2000).
8. J. A. Wright and Y. C. Tai, in *Proceedings of the 46th Annual International Relay Conference–NARM'98*, Oak Brook, Illinois, 13-1, April (1998).
9. J. W. Judy, R. S. Muller, and H. H. Zappe, *J. Microelectromech. Syst.*, **4**, 162 (1995).
10. S. Kawahito, Y. Sasaki, M. Ishida, and T. Nakamura, Digest Tech. Papers, Transducers 93' 888 (1993).
11. W. Daniau, S. Ballandras, L. Kubat, J. Hardin, G. Martin, and S. Basrour, *J. Micromech. Microeng.*, **5**, 270 (1995).
12. S. A. Watson, Ni Development Institute Tech. Series Reports 10047–10055 (1998).
13. S. K. Ghost, A. K. Grover, G. K. Dey, and M. K. Totlani, *Surf. Coat. Technol.*, **126**, 48 (2000).
14. S. E. Hadian and D. R. Gaba, *Surf. Coat. Technol.*, **122**, 118 (1999).
15. J. C. Sadak and F. K. Sautter, *J. Vac. Sci. Technol.*, **11**, 771 (1974).
16. Z. Chen, X. Xu, C. C. Wong, and S. Mhaisalkar, *Surf. Coat. Technol.*, **167**, 170 (2003).
17. J. L. Marti, *Plating*, **53**, 61 (1966).
18. W. H. Safranek, *The Properties of Electrodeposited Metals and Alloys*, American

Electroplaters and Surface Finishers Society, Orlando, FL (1986).
19. Y. Tsuru, M. Nomura, and F. R. Foulkes, *J. Appl. Electrochem.*, **30**, 231 (2000).
20. Y. Tsuru, M. Nomura, and F. R. Foulkes, *J. Appl. Electrochem.*, **32**, 629 (2002).
21. R. V. Shenoy and M. Datta, *J. Electrochem. Soc.*, **143**, 544 (1996).
22. J. K. Luo, D. P. Chua, A. J. Flewitt, S. M. Spearing, N. A. Fleck, and W. I. Mline, *J. Electrochem. Soc.*, **152**, C36 (2005).
23. W. Fang and J. A. Wickert, *J. Micromech. Microeng.*, **6**, 301 (1996).
24. M. Gad-el-Hak, *The MEMS Handbook*, CRC Press, New York (2001).
25. J. H. He, J. K. Luo, H. R. Le, and D. F. Moore, Proceedings SPIE, 5836, 208, Seville, Spain May (2005).
26. J. K. Luo, A. J. Flewitt, S. M. Spearing, N. A. Fleck, and W. I. Milne, *Mater. Lett.*, **58**, 2306 (2004).
27. J. Ruythooren, K. Attenborough, S. Beerten, P. Merken, J. Fransaer, E. Beyne, C. V. Hoof, J. D. Boeck, and J. P. Celis, *J. Micromech. Microeng.*, **10**, 101 (2000).
28. Alfa Aesar Catalog "Research Chemicals, Metals and Materials," p. 945 (2004).
29. W. H. Sufranek, *J. Vac. Sci. Technol.*, **11**, 765 (1974).
30. J. W. Gardner, V. K. Varadan, and O. O. Awadelkarim, *Microsensors MEMS and Smart Devices*, John Wiley & Sons Ltd., New York (2001).
31. S. C. Chang, J. M. Shieh, B. T. Dai, M. S. Feng, and Y. H. Li, *J. Electrochem. Soc.*, **149**, G535 (2002).
32. N. S. Qu, D. Zhu, K. C. Chan, and W. N. Lei, *Surf. Coat. Technol.*, **168**, 123 (2003).
33. W. Fang, C. H. Lee, and H. H. Hu, *J. Micromech. Microeng.*, **9**, 236 (1999).
34. M. G. Allen, M. Mehregany, R. T. Howe, and S. D. Senturia, *Appl. Phys. Lett.*, **51**, 241 (1987).
35. J. Zhang, *J. Mater. Process. Technol.*, **123**, 329 (2002).
36. I. Tabakovic, S. Reimer, V. Inturi, P. Jallen, and A. Thayer, *J. Electrochem. Soc.*, **147**, 219 (2000).
37. N. S. Qu, D. Zhu, K. C. Chan, and W. N. Lei, *Surf. Coat. Technol.*, **168**, 123 (2003).
38. B. W. Sheldon, K. H. A. Lau, and A. Rajumani, *J. Appl. Phys.*, **90**, 5097 (2001).
39. F. A. Doljack and R. W. Hoffman, *Thin Solid Films*, **12**, 71 (1972).
40. L. S. Stephens, K. W. Kelly, S. Simhadri, A. B. McCandless, and E. I. Meletis, *J. Microelectromech. Syst.*, **10**, 347 (2001).
41. H. Guckel, T. Randazzo, and D. W. Burns, *J. Appl. Phys.*, **57**, 1671 (1985).
42. S. Pamidighantam, R. Puers, K. Baer, and H. A. Tilmans, *J. Micromech. Microeng.*, **12**, 458 (2002).